

# Catalysis Science & Technology

Accepted Manuscript



This is an *Accepted Manuscript*, which has been through the Royal Society of Chemistry peer review process and has been accepted for publication.

*Accepted Manuscripts* are published online shortly after acceptance, before technical editing, formatting and proof reading. Using this free service, authors can make their results available to the community, in citable form, before we publish the edited article. We will replace this *Accepted Manuscript* with the edited and formatted *Advance Article* as soon as it is available.

You can find more information about *Accepted Manuscripts* in the [Information for Authors](#).

Please note that technical editing may introduce minor changes to the text and/or graphics, which may alter content. The journal's standard [Terms & Conditions](#) and the [Ethical guidelines](#) still apply. In no event shall the Royal Society of Chemistry be held responsible for any errors or omissions in this *Accepted Manuscript* or any consequences arising from the use of any information it contains.



Journal Name

ARTICLE

## Simultaneous investigation of the structure and surface of a Co/alumina catalyst during Fischer-Tropsch synthesis: Discrimination of various phenomena with beneficial or disadvantageous impact on activity

Received 00th January 20xx,  
Accepted 00th January 20xx

DOI: 10.1039/x0xx00000x

www.rsc.org/

Julien Scalbert<sup>a,\*</sup>, Isabelle Cléménçon<sup>a</sup>, Philippe Lecour<sup>a</sup>, Laure Braconnier<sup>a</sup>, Fabrice Diehl<sup>a</sup>, Christèle Legens<sup>a</sup>

A system combining XRD and DRIFTS characterization techniques was developed to monitor the structure and the surface of a cobalt catalyst during the Fischer-Tropsch synthesis. In the present study, several phenomena could be observed and discriminated. Firstly, residual cobalt oxide was found to further reduce during the reaction, but this enhancement in reduction degree did not clearly lead to a gain in activity. Secondly, the formation of linear and bridged carbonyls took place rapidly at the surface of the catalyst. A surprising increase in activity was observed while the concentration in carbonyls was decreasing, supporting the idea that CO dissociation was a crucial step in the Fischer-Tropsch mechanism. Arising from that, the increase in activity was attributed to a surface reconstruction transforming sites favoring CO strong adsorption into sites active for CO dissociation. Finally, most of the catalyst deactivation was assigned to the formation of surface oxygenate species, which were suspected to result from the reduction of CoO with hydrocarbons.

### Introduction

The question of energy is a crucial point in our modern societies. Petroleum remains up to date the essential source in the production of liquid fuels for transportation. Nevertheless, the exponential needs in petroleum combined with the ineluctable depletion of this geostrategic resource require urgently alternatives allowing fuel production from diversified sources. Fischer-Tropsch process offers the possibility to synthesize high-quality hydrocarbons from synthesis gas obtained from various sources such as coal, natural gas, and promisingly renewable biomass. Because of their efficiency for the production of high molecular weight n-alkanes, and of their large availability and versatility, alumina-based cobalt catalysts have received a lot of attention both in academic and industrial research<sup>1-2</sup>.

The mechanism of the Fischer-Tropsch synthesis as well as the possible phenomena leading to catalyst deactivation are however still unclear and subject to intense discussions<sup>3-5</sup>. If it is now generally accepted that the Fischer-Tropsch mechanism can be described as a polymerization reaction, there is no consensus on the nature of the monomer nor on the way in which chain growth takes place<sup>3</sup>. Various complex

mechanisms which could be classified into two categories have been proposed: (i) mechanisms based on the dissociation of CO at the surface of the catalyst followed by the hydrogenation of individual carbon into CH<sub>2</sub> species which can then combine to form oxygen-free hydrocarbon products, (ii) mechanisms based on the hydrogenation of molecularly adsorbed CO, and possibly involving direct CO insertion during the chain growth, thus forming oxygenate intermediates. Just as there are several postulates concerning the Fischer-Tropsch mechanism, there are also many hypotheses to explain the deactivation occurring during the reaction. Among them, cobalt oxidation by water is one of the most contentious. While some authors showed the formation of cobalt oxide after Fischer-Tropsch synthesis<sup>6</sup>, some other concluded that oxidation could not occur under realistic Fischer-Tropsch conditions<sup>7-8</sup>. However, it appears that these two opposite points of view could be reconciled, in that the oxidation of cobalt should likely depend on several parameters such as the particle size, support, promoters, rate of conversion and thus water content and H<sub>2</sub>/H<sub>2</sub>O ratio. Besides, water is also suspected to assist sintering and agglomeration of cobalt particles<sup>8-9</sup>, classically proposed to be responsible for a part of deactivation<sup>5</sup>. Apart from poisoning by syngas contaminants, deactivation can also result from carbon deposition and fouling<sup>5</sup>. Metal surface reconstruction was also proposed to be a cause of deactivation<sup>10</sup>. However, one can imagine that such a reconstruction could also have a beneficial effect if it leads to the creation of new active sites from previously inactive or inaccessible ones. Yet, better understanding the

<sup>a</sup> IFP Energies nouvelles, Rond-point de l'échangeur de Solaize, BP 3, 69360 Solaize, France.

\* Corresponding author: dr.julien.scalbert@gmail.com (J. Scalbert).

† Electronic Supplementary Information (ESI) available: TEM and magnetism measurements; conversion, selectivity, yield and TOF calculations; estimation of reduction degree. See DOI: 10.1039/x0xx00000x

reaction mechanism and unraveling the origins of deactivation are of fundamental importance to improve catalyst stability while keeping a high activity and selectivity to products of interest.

The recent development of *operando* methodology combining catalyst characterization during reaction and simultaneous catalytic properties measurements has opened new ways for evidencing and understanding phenomena occurring during catalytic reactions, and in particular some of those inducing deactivation<sup>11-12</sup>. With the hopeful goal to find relationships between structural, surface and catalytic properties of cobalt catalysts, we have developed an innovative XRD-DRIFTS prototype allowing *operando* characterizations under realistic Fischer-Tropsch conditions.

## Experimental

### Catalyst synthesis and *ex situ* characterization

A model Co/Al<sub>2</sub>O<sub>3</sub> catalyst with a metal loading of 13.2 wt % was prepared by Co(NO<sub>3</sub>)<sub>2</sub> incipient wetness impregnation on  $\gamma$ -alumina (Puralox<sup>®</sup> SCCa, Sasol Germany GmbH, with a surface area of 170 m<sup>2</sup>.g<sup>-1</sup> and a pore volume of 0.45 cm<sup>3</sup>.g<sup>-1</sup>) according to a classical method already reported<sup>13</sup>. After drying overnight at 85 °C, the material was calcined at 400 °C during 4 hours under air flow.

Cobalt loading was checked by wavelength dispersive X-ray fluorescence (XRF). Transmission electron microscopy (TEM) was used to estimate the average cobalt particle size and subsequently the cobalt dispersion. *In situ* magnetic measurements were carried out as previously detailed<sup>13</sup>, to determine the reduction degree of the catalyst after reduction at 500 °C.

### Catalytic tests and XRD-DRIFTS *operando* characterization

To perform the *operando* study, about 230 mg of the Co/Al<sub>2</sub>O<sub>3</sub> catalyst was placed on a quartz fritted disk inside the reaction cell of the XRD-DRIFTS prototype (Figure 1) and reduced at 500°C during 16 hours under a flow of 1 L.h<sup>-1</sup> of pure H<sub>2</sub>. Before switching to an H<sub>2</sub>+ CO feed (Fischer-Tropsch synthesis), the cell was cooled down to 220 °C, flushed with N<sub>2</sub> and the pressure was increased to 6 bars. The catalytic test was then carried out at 220 °C, 6 bar, under a 1.5 L.h<sup>-1</sup> flow made of H<sub>2</sub> and CO in a mixture molar ratio H<sub>2</sub>/CO of 2. All the lines, as well as the base of the cell, were kept at 120 °C to limit the condensation of reaction products. In addition, the reaction conditions were experimentally defined so that the CO conversion was kept around 10 % and the total gas flow was able to carry the heaviest waxes with the outlet gas.

The reaction cell was especially designed to carry out catalytic reactions in a fixed-bed-like configuration, while simultaneously characterizing the structure of the catalyst with X-Ray Diffraction (XRD) and its surface with Diffuse Reflectance Infrared Fourier Transform Spectroscopy (DRIFTS). The XRD part of the apparatus consists in an INEL diffractometer in a Debye-Scherrer configuration, with a molybdenum tube (wavelength  $\lambda_{\text{K}\alpha 1} = 0.7090 \text{ \AA}$ ) in transmission mode and an INEL CPS 120 curved detector. The beryllium windows on the path

of the X-ray beam allow transmitting it while maintaining the sealing and the resistance of the reaction cell, specified to be used under pressure up to 18 bar.

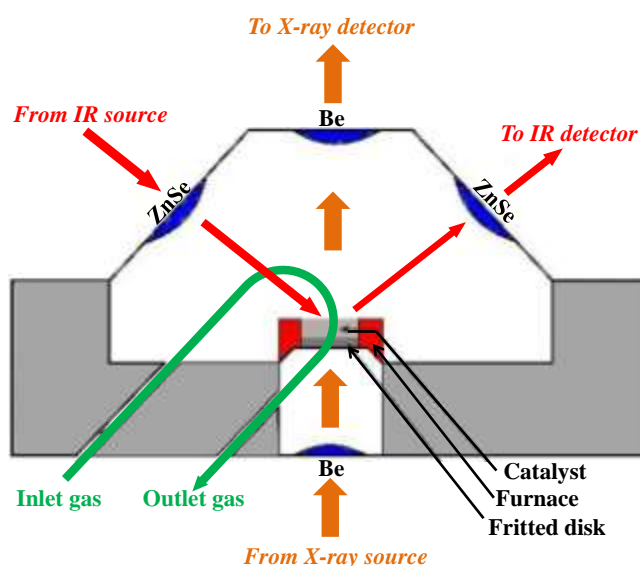


**Figure 1.** Picture of the XRD-DRIFTS apparatus (top) and scheme of the reaction cell (bottom).

*Operando* X-ray measurements were carried out every 4 hours with a duration record of 1 hour. The DRIFTS part of the apparatus consists in a Bruker IRcube OEM FT-IR with a MCT (Mercury-Cadmium-Telluride) detector cooled at -196 °C. A set of mirrors in an appropriate geometric configuration allows the reflection of the IR beam from the source to the surface of the sample where the subsequent diffuse IR radiation is then reflected to the detector. Thick ZnSe windows are used to allow an optimal transmission of the IR beam while also maintaining the sealing and the resistance of the cell. To prevent any damage due to the high operating temperature,

ZnSe windows were maintained at 70 °C, while the temperature of the cell walls was 110 °C at least during Fischer-Tropsch synthesis. To limit the influence of CO present in the gas phase of the cell on the DRIFTS signal, the total pressure for the reaction was limited to 6 bar. *Operando* DRIFT spectra were recorded during 3.6 minutes (2048 scans) at different times of the reaction and plotted in units of logarithm inverse reflectance. The DRIFT spectrum of the catalyst before the beginning of the reaction was used as background for the subsequent DRIFT spectra recorded during Fischer-Tropsch synthesis.

The outlet gas was analyzed on-line by gas chromatography (GC). Hydrocarbons were separated using a PONA column and detected with a flame ionization detector (FID). The detection and quantification of CO, CO<sub>2</sub> and N<sub>2</sub> were performed using PPU and MS5A columns with a thermal conductivity detector (TCD), while PPQ and MS5A columns associated with another TCD allowed H<sub>2</sub> quantification.

The conversion was defined as CO conversion, and selectivity was calculated on a carbon molar basis (details of the calculations are provided in the Supporting Information). The turnover frequency (TOF) was defined as the molar quantity of converted CO per mole of surface cobalt atoms per second. The number of accessible surface cobalt atoms was directly estimated from cobalt loading and dispersion. A corrected TOF taking into account the reduction degree of the catalyst was also calculated, assuming that the global reduction degree was similar both in the bulk and at the surface of the cobalt particles (see Supporting Information).

## Results

### Ex situ characterization

The main useful data obtained from ex situ characterizations are shown in Table 1.

**Table 1.** Properties of the studied Co/Al<sub>2</sub>O<sub>3</sub> catalyst

Co loading (wt%)	Particle size (nm)	Dispersion (%)	Co surface atoms (mmol.g <sub>catal</sub> <sup>-1</sup> )	Reduction degree at 500 °C (%)
13.2	9.9	9.7	0.22	68
± 0.6	± 1.0			± 10

### Catalytic properties

The CO conversion was followed with time on stream for 8 days. During the first hours of the reaction, the syngas mixture was progressively replacing N<sub>2</sub> in the reaction cell, and the N<sub>2</sub> content in the outlet flow was below 2 % after three hours as measured with GC. The conversion showed a particular profile which could be easily decomposed in three different periods:

first period when conversion is reaching a maximum (from 0 to 2 days), a second period when conversion is rapidly decreasing to a minimum (from 2 to 5 days), and a third period when conversion is more or less stable (Figure 2).

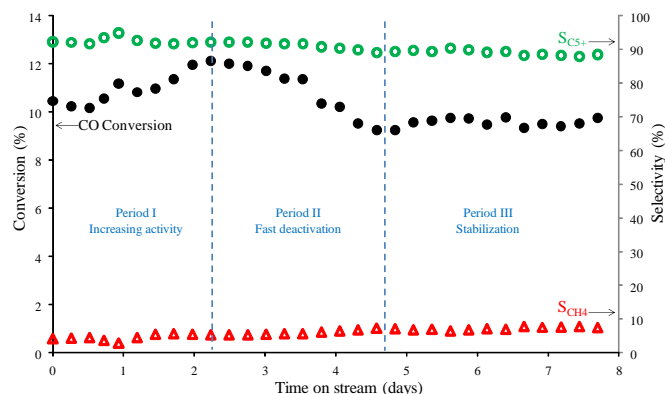


**Figure 2.** CO conversion (●) and selectivity in CH<sub>4</sub> (Δ) and C<sub>5+</sub> (○) as a function of time on stream, over Co/Al<sub>2</sub>O<sub>3</sub> catalyst at 220 °C, 6 bar, H<sub>2</sub>/CO = 2.

The arbitrary described first and second periods could also be seen as an intermediate stage before the third period which could be then seen as a permanent regime with slow deactivation. At the end of the test, *i.e.* after 8 days on stream, the TOF was stable, around 12.5 mmol<sub>CO</sub>.mol<sub>Co<sub>surf</sub></sub><sup>-1</sup>.s<sup>-1</sup>. Taking into account a reduction degree of 87 % determined by XRD after 8 days on stream (see the following parts), the corrected TOF was about 14.9 mmol<sub>CO</sub>.mol<sub>Co<sub>surf</sub></sub><sup>-1</sup>.s<sup>-1</sup>. It is worth noting that these values are right in the range of those already reported for most typical Fischer-Tropsch cobalt catalysts in similar conditions<sup>14-15</sup>.

Regarding products selectivity, the Co/Al<sub>2</sub>O<sub>3</sub> catalyst showed a very high C<sub>5+</sub> selectivity which however slightly decreased from 92 to 88 % in favor of methane selectivity which in the same time increased from 4 to 7 %. Again, those values are very similar to those already reported in similar conditions<sup>16-17</sup>. The catalytic properties exhibited by the model catalyst in the *operando* system are thus in very good agreement with those obtained by research teams working with classical fixed-bed reactors. And therefore, although spectroscopic reaction cells are of course by no means ideal reactors<sup>10-11</sup>, we can fairly consider that the behavior of the *operando* cell is similar enough to that of fixed-bed reactors, thus justifying the relevance of the following results.

### XRD *operando* characterization

*Operando* XRD allowed monitoring the evolution of the catalyst structure during the reaction (Figure 3).

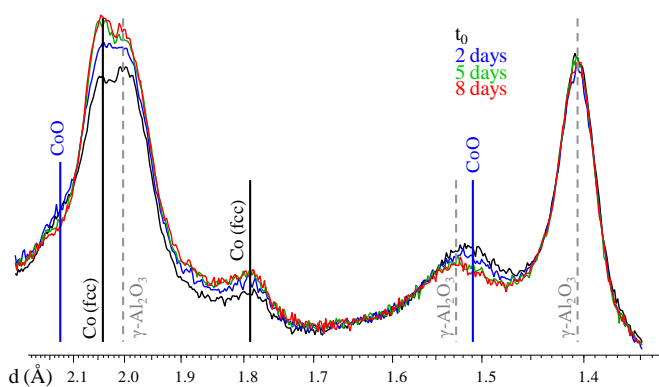


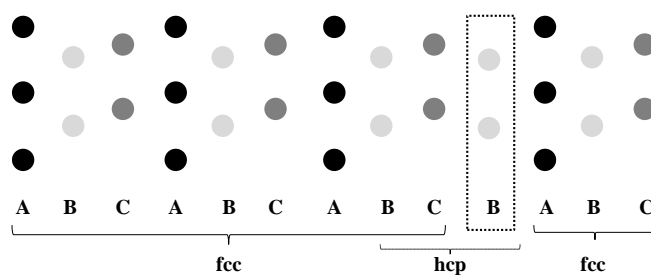
**Figure 3.** *Operando* XRD diffraction patterns of Co/Al<sub>2</sub>O<sub>3</sub> catalyst recorded during Fischer-Tropsch synthesis at 220 °C, 6 bar, H<sub>2</sub>/CO = 2.

After *in situ* reduction, three different crystalline phases are observed on the X-ray diagrams: face-centered cubic metal cobalt (fcc Co) with its typical peaks at d-spacing around 2.05 and 1.77 Å, CoO with its main peaks at 2.13 and 1.51 Å, and  $\gamma$ -Al<sub>2</sub>O<sub>3</sub> with peaks at 1.98-2.00, 1.54 and 1.40-1.41 Å. The proportion of CoO was estimated from the area of its peak at 1.51 Å, considering as reference the X-ray diagram obtained during activation when CoO was the only observed cobalt-containing phase (details are provided in the Supporting Information). After reduction, CoO content among the cobalt-containing phases was 30 % ( $\pm$  10 %), and by deduction fcc Co content was 70 % ( $\pm$  10 %). This was confirmed by the reduction degree of 68 % determined by magnetic measurements at 500 °C.

During the first five days of the reaction, the intensity of the diffraction peaks at 2.05 and 1.77 Å assigned to fcc Co increased. In parallel, the intensity of the peaks at 2.13 and 1.51 Å assigned to CoO decreased. From this, it is obvious that a part of residual CoO was further reduced into fcc Co during the reaction. This observed enhanced reduction is in agreement with the suggestions of several authors claiming that the Fischer-Tropsch reaction conditions favor cobalt reduction rather than oxidation<sup>5,7</sup>.

Considering the shape and the width of the peaks assigned to fcc Co, it is worth noting that an asymmetric broadening of these two peaks occurred during the reaction. A global symmetric broadening would mean that the coherent domain size of the fcc crystallites decreases with time on stream, and by extension could be an argument against the hypothesis of any crystallite sintering during the test. However, the broadening is here clearly asymmetric and particularly marked in the region between the peaks at 2.05 and 1.77 Å. This could be attributed to the appearance of defects such as stacking faults which could locally be defined as hexagonal close packed (hcp) stacking into the fcc crystalline structure (**Scheme 1**).

Although no peak associated with hcp Co is detectable on the *operando* diffraction patterns, the region where the broadening occurs seems indeed to be centered around 1.91 Å (**Figure 4**) which is typically assigned to hcp Co (101) diffraction peak.



**Scheme 1.** Representation of stacking faults between fcc and hcp crystallographic phases.

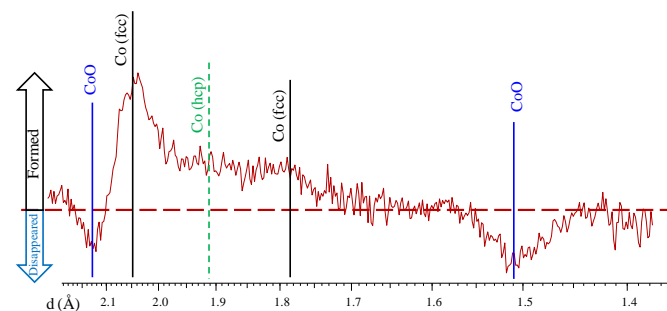


**Figure 4.** Diffraction pattern obtained after subtraction of the *operando* X-ray diagrams obtained after and before Fischer-Tropsch synthesis over Co/Al<sub>2</sub>O<sub>3</sub> catalyst.

Note that it cannot be excluded that this global asymmetric broadening assigned to defects formation might also hide a lesser symmetric broadening which would be due to a decrease in the crystallite size, or on the opposite a lesser symmetric narrowing which would be then ascribed to sintering.

No diffraction peak which could have been assigned to other crystalline phases such as cobalt carbide or graphite was observed on *operando* X-ray diffraction patterns, thus suggesting that these compounds were not formed during the test, or at least that their concentration was below the detection limit (< 5 %). It is important to underline that XRD is a bulk technique and thus not suitable to detect tiny changes, in particular at the surface of the material. Thus the formation of cobalt carbide, in particular in an amorphous state, or the formation of amorphous carbon compounds at the surface of the catalyst cannot be ruled out.

#### DRIFTS *operando* characterization

Using DRIFTS as a complementary *operando* technique allowed observing the surface of the catalyst during the reaction (**Figure 5**). As already stated by Meunier<sup>11</sup>, the use of differential conditions (conversion around 10 % or less) enables both qualitative and quantitative (at least semi-quantitative) analysis of DRIFT spectra.

Various IR bands corresponding to various species appear and evolve with time on stream. The saturation of the bands at 2180 and 2110 cm<sup>-1</sup> assigned to CO in gas phase<sup>18</sup> is due to the high concentration of CO in the cell, *i.e.* a CO partial pressure

of 2 bars, combined to a long optical path of several centimeters through the cell.

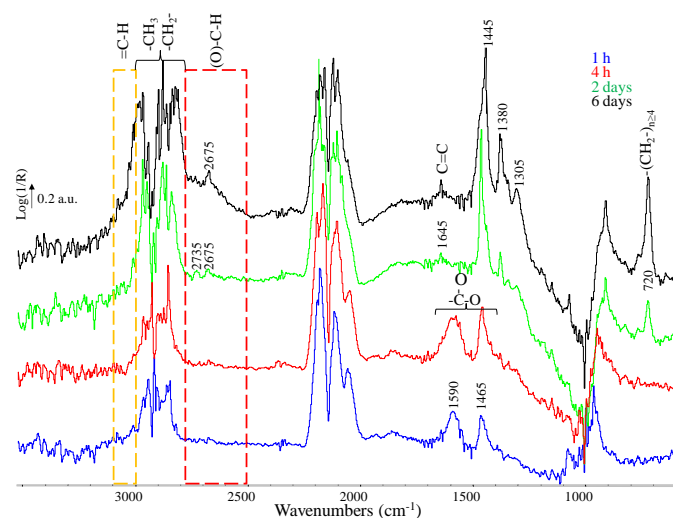


**Figure 5.** *Operando* DRIFT spectra of the surface of Co/Al<sub>2</sub>O<sub>3</sub> catalyst recorded during Fischer-Tropsch synthesis at 220 °C, 6 bar, H<sub>2</sub>/CO = 2 (after subtraction of the initial DRIFT spectrum at t<sub>0</sub> as a background and of a reference spectrum of 1 bar of pure CO).

In the O-H vibration region between 3700-3200 cm<sup>-1</sup>, no clear signal can be identified, but noise likely due to the presence of water, the main reaction product which is also identified by its rotovibrational components centered at 1590 cm<sup>-1</sup>. Note that these bands assigned to gaseous water may also be due to moisture variations in the outside air.

Several complex bands are observed in the 2500-3100 cm<sup>-1</sup> region. The bands between 2800 and 3000 cm<sup>-1</sup> can be assigned to stretching vibrations of methyl and methylene groups belonging to various hydrocarbons<sup>19</sup>. The intensity of these bands increases with time on stream, which means that the surface of the catalyst is more and more covered with hydrocarbons species. This is confirmed by the bands at 1445, 1455, 1380 and 1470 cm<sup>-1</sup> which could be assigned to deformation vibrations of -CH<sub>3</sub> and -CH<sub>2</sub>- groups<sup>19</sup>. Moreover, a new band at 720 cm<sup>-1</sup> appears and increases after 36 hours on stream. This band is typical of δ(C-H) out-of-plane vibration from methyl groups when more than four -CH<sub>2</sub>- are directly connected in the carbon chain<sup>19</sup>. This should mean that adsorbed hydrocarbons on the catalyst surface are growing up during the reaction.

It is important to point out that methane, with its typical rotovibrational bands centered at 3016 and 1305 cm<sup>-1</sup>, is not detected in the gas phase of the *operando* cell whereas it is the first hydrocarbon reaction product as measured by GC. This indicates that gaseous products back-diffusion is fairly well minimized and confirms that the hydrodynamics of the reaction cell behaves as expected in a fixed-bed reactor. By the way, no liquid or solid product was observed on the ZnSe windows, which could have though constituted a cold point of

the reaction cell. In particular, IR spectra recorded with a mirror in lieu of the sample revealed that the ZnSe windows were still perfectly clean after reaction. Thus it is rather unlikely that some of IR bands might be assigned to hypothetical products which would condense in the cell during the reaction. The band in the 3000-3080 cm<sup>-1</sup> region, also increasing with time on stream, could be assigned to the ν(C<sub>sp2</sub>-H) vibration from not fully substituted alkenes<sup>19</sup>. The thin band emerging at 1645 cm<sup>-1</sup> could then be assigned to the double bond C=C vibration<sup>19</sup>. Bands between 3000 and 3100 cm<sup>-1</sup> could also have been attributed to the ν(C<sub>sp2</sub>-H) vibration from aromatics. In this case, a set of intense bands corresponding to the aromatic ring vibrations should appear around 1600 and 1500 cm<sup>-1</sup>. In the first hours of the reaction, intense bands at 1590 and 1465 cm<sup>-1</sup> could have been assigned to these aromatic rings, but at that time the bands in the 3000-3100 cm<sup>-1</sup> region are almost nonexistent. And after 2 days on stream, when ν(C<sub>sp2</sub>-H) vibration is clearly detected, the band at 1590 cm<sup>-1</sup> has disappeared or at least its intensity has strongly decreased. This contradiction seems to exclude aromatics formation in the present case. Moreover, the large bands at 1590 and 1465 cm<sup>-1</sup> observed at the early edges of the reaction are more likely assigned to carboxylate species<sup>11</sup>. The presence of formates is also suggested by the presence of the bands near 1380, 1590, 2740 and 2890 cm<sup>-1</sup>.

The large band between 2770 and 2500 cm<sup>-1</sup> emerging after several days on stream is more difficult to assign and is likely due to organic compounds containing a heteroatom, namely oxygen. It may be associated with C-H vibration from CHO group of aldehydes, generally observed between 2650 and 2870 cm<sup>-1</sup>.<sup>20</sup> The presence of carboxylic acid species is not excluded. The low-frequency wing in the 2700-2500 cm<sup>-1</sup> region is indeed typical of carboxylic acids, due to overtones and combination bands near 1440 and 1300 cm<sup>-1</sup> (then assigned to OH bend and C-O stretch respectively) enhanced by Fermi resonance with the broad band centered at 3000 cm<sup>-1</sup> (OH stretch in the case of carboxylic acid dimer form)<sup>20</sup>. However, in both cases, no well-defined peak can be clearly assigned to the C=O vibration in aldehydes or carboxylic acids<sup>20</sup>, but the large broad band observed in the 1650-1800 cm<sup>-1</sup> region might consist in several superimposed bands associated with C=O vibrations from various complex oxygenates species. It is thus very hazardous to distinguish and identify the real nature and composition of such presumed and probably complex oxygenate species.

Negative bands between 900 and 1300 cm<sup>-1</sup> are also observed on the *operando* spectra. These large negative bands, whose absolute intensity increases with time on stream, are related to the alumina support<sup>12</sup> and reveal that the support is step by step covered with other species. Among them, adsorbed hydrocarbons and oxygenates could be responsible for this covering, as they are observed on the spectra. However, the presence of infrared-transparent species such as atomic carbon, amorphous polymeric carbon or graphene could not be ruled out, as already suggested in a similar study<sup>21</sup>.

DRIFT *operando* spectra also brought out the formation of cobalt-carbonyl species at the surface of the catalyst (Figure 6).

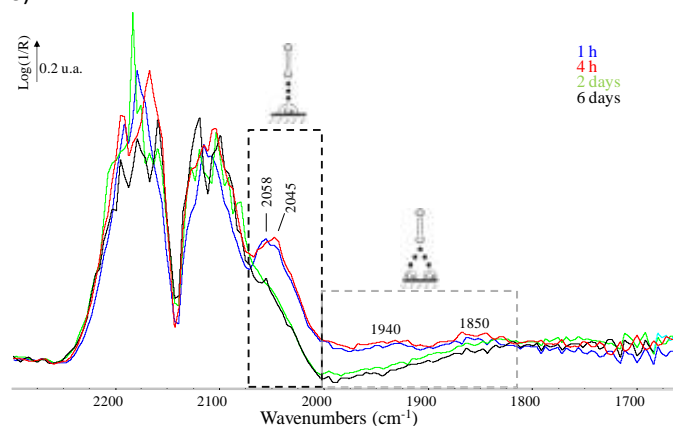


**Figure 6.** *Operando* DRIFT spectra of the surface of Co/Al<sub>2</sub>O<sub>3</sub> catalyst recorded during Fischer-Tropsch synthesis at 220 °C, 6 bar, H<sub>2</sub>/CO = 2. Zoom in carbonyl region, after subtraction of a reference spectrum of 1 bar of pure CO.

The band at 2058 cm<sup>-1</sup> and the shoulder at 2045 cm<sup>-1</sup> can be assigned to linear carbonyls on metal cobalt, and the large bands centered around 1940 and 1850 cm<sup>-1</sup> can be assigned to bridged carbonyls<sup>18,22</sup>. All these bands appear rapidly at the early beginning of the reaction. Their intensity reaches a maximum after a few hours on stream and then decreases to a minimum. It may suggest a first increase and a subsequent decrease in the number of active sites for CO adsorption. Several phenomena could be responsible for this evolution as exposed in the following discussion.

## Discussion

The XRD *operando* characterization revealed an enhanced reduction of the catalyst during the first days of Fischer-Tropsch synthesis, which is in agreement with previous reports<sup>5,7</sup>. Unfortunately it did not automatically result in an enhanced catalytic activity. Except at the early edge of the reaction when conversion and yield in C<sub>5+</sub> reached a maximum (first period), which may be related to the creation of new active sites by the further reduction of CoO into Co, the next periods exhibited deactivation (Figure 7).

Moreover, the period with the highest conversion of residual CoO into Co takes place almost exactly at the same time as the fast catalyst deactivation does (second period). So either this enhanced reduction does not generate new active sites for Fischer-Tropsch synthesis, which could be the case if the reduction occurs inside the core of the particles for instance, whether this generation is not important enough to compensate opposite deactivation phenomena.

As previously stated, the reduction of residual CoO into Co is accompanied with the creation of crystalline defects. This defects formation could be harmful, generating inactive sites from previously inactive oxidized sites but also from previously

active metallic sites since stacking faults would induce changes in the neighborhood of the cobalt atoms.

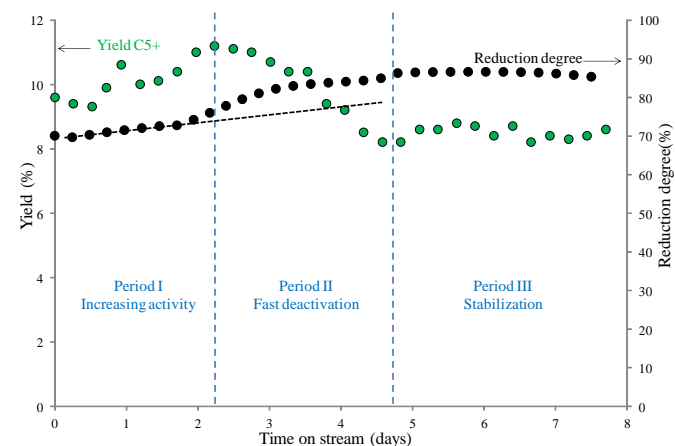


**Figure 7.** C<sub>5+</sub> yield (●) and reduction degree of the catalyst (●) as a function of time on stream during Fischer-Tropsch synthesis at 220 °C, 6 bar, H<sub>2</sub>/CO = 2.

Besides that, even if the XRD data show a global asymmetric broadening of the peaks assigned to Co, sintering of cobalt crystallites cannot be ruled out. Cobalt agglomeration was indeed already evidenced and associated with deactivation over a very similar catalyst though in a slurry reactor<sup>23</sup>. Future *in situ* TEM experiments could help in clarifying this point. In parallel, DRIFTS *operando* characterization showed several crucial points. Linear and bridged carbonyls were formed on metal cobalt sites and the evolution of their corresponding areas on DRIFT spectra (determined by integration of the 2000-2070 cm<sup>-1</sup> and 1810-2000 cm<sup>-1</sup> regions respectively) is reported in Figure 8.

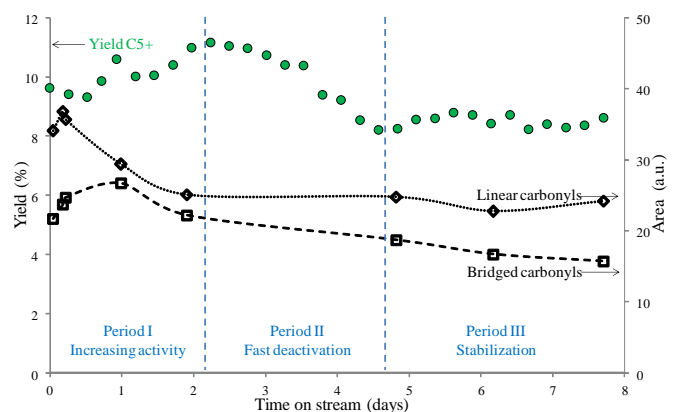


**Figure 8.** C<sub>5+</sub> yield (●) and linear (◇) and bridged (□) carbonyls IR areas as a function of time on stream during Fischer-Tropsch synthesis at 220 °C, 6 bar, H<sub>2</sub>/CO = 2.

As previously described, both linear and bridged carbonyls reach a maximum surface concentration at the beginning of the reaction before an ultimate decrease, but their evolution is not synchronous. The first hours of carbonyls formation might be simply related to the kinetics of CO adsorption and the necessary time to achieve an equilibrium and a maximum coverage at the catalyst surface. Since the formation of

carbonyls strongly depends on CO partial pressure<sup>22</sup>, it is important to mention that N<sub>2</sub> was completely replaced by syngas in the cell within four hours. The increase in carbonyls could also result from the creation of new metal sites by the reduction of remaining CoO, as this phenomenon was evidenced by *operando* XRD characterization. It might also suggest a possible enhanced dispersion of the metal phase during the first edges of the reaction, but it is important to remind that no change related to particle size was observed on diffraction diagrams.

On the contrary, the decrease in carbonyls is likely due to a decrease in the number of sites favoring CO adsorption and which could result from many causes such as (i) cobalt sintering, (ii) cobalt oxidation, (iii) cobalt carbide formation, (iv) covering by adsorbed intermediates and heavy by-products, and (v) surface reconstruction<sup>24-25</sup>. However, the expressed four first possible causes should lead to a catalyst deactivation, which is clearly not the case during the first period when activity increases to a maximum. Surface reconstruction is the only hypothesis not necessarily linked to deactivation. Technically, a surface reconstruction is a phenomenon which involves rearrangements and displacements of surface atoms and induces changes in the geometry, periodicity and symmetry of the surface<sup>26-28</sup>. The reconstruction of the metallic phase could favorably change the reactivity of metal sites by modifying their geometric configuration and number of coordination. Initially inactive sites can thereby become active for Fischer-Tropsch synthesis, thus explaining the observed enhanced activity. Explicitly, some sites initially favoring CO linear adsorption can be transformed into different sites favoring new interactions such as CO bridged adsorption during the first day of the test, and above all into sites favoring CO dissociation.

This approach is consistent with the hypothesis that Fischer-Tropsch mechanism involves the dissociation of carbon monoxide<sup>3-4</sup>. Cobalt active sites for Fischer-Tropsch synthesis would then be those favoring the dissociation of CO and not those favoring its stabilization by molecular adsorption without further breaking of the C-O bond. A recent work by Tuxen and coworkers has demonstrated that CO molecules dissociate much more efficiently on larger (15 nm) than on smaller (4 nm) nanoparticles<sup>29</sup>. This could be directly related to the coordination number of cobalt atoms. High-coordination metal sites constituting the major part of surface sites of large particles would then be identified as the active sites favoring CO dissociation, whereas low-coordination sites present in higher proportion in smaller particles would rather favor CO molecular adsorption. The beneficial surface reconstruction occurring at the beginning of the reaction would thus lead to more sites of high coordination number, such as dense plans, at the expense of low-coordination sites such as edges or corners. Our proposition is also in agreement with the well-known fact that small cobalt nanoparticles below 6 nm, *i.e.* with a majority of low-coordination sites, exhibit a lower Fischer-Tropsch activity than larger ones<sup>29-30</sup>.

Various adsorbed species were observed on *operando* DRIFTS spectra and among them oxygenated and unsaturated species

seem to be mostly formed during the fast deactivation period, as suggested by the evolution of their respective areas (determined by integration of the 2480-2820 cm<sup>-1</sup> and 3000-3100 cm<sup>-1</sup> regions respectively) illustrated on **Figure 9**.

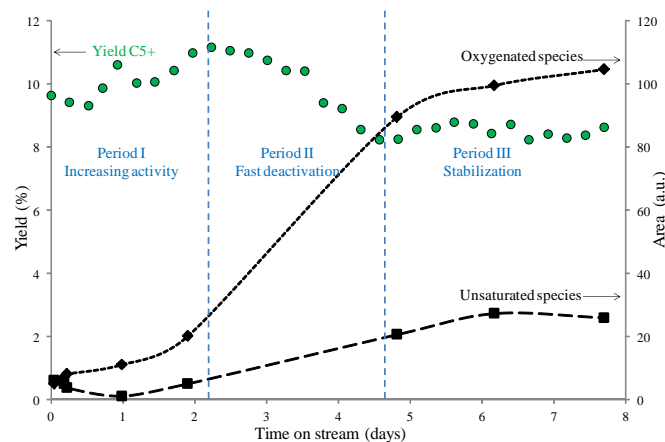


**Figure 9.** C<sub>5+</sub> yield (●) and IR areas of oxygenated (■) and unsaturated (◆) species adsorbed at the surface of the catalyst as a function of time on stream during Fischer-Tropsch synthesis at 220 °C, 6 bar, H<sub>2</sub>/CO = 2.

These strongly adsorbed species could likely be responsible for the catalyst deactivation by covering active sites. Unsaturated species should result from an incomplete hydrogenation of reaction intermediates into alkanes or from the competitive dehydrogenation of the latter into alkenes. Oxygenated species formation is more vague. The mechanism consisting in CO insertion can explain the formation of oxygenated intermediates and byproducts such as alcohols, ketones, aldehydes and carboxylic acids<sup>3-4</sup>. Hydroformylation reaction could also occur over cobalt between CO and alkenes byproducts leading to aldehydes<sup>31</sup>.

It is worth noting that the fast formation of oxygenated adsorbed species occurs in the present case at the same time as does the most part of the CoO reduction into Co (Figures 7 and 9). It would be easy to suppose that CoO was directly reduced from H<sub>2</sub> at 220 °C, but it is also hard to explain it as this refractory CoO was stable during reduction under pure H<sub>2</sub> at 500 °C during 16 hours. That is the reason why we propose here that the residual CoO was not directly reduced from H<sub>2</sub> during Fischer-Tropsch synthesis, but was involved in oxidation reactions of hydrocarbon products leading to metal Co and strongly adsorbed oxygenate products, possibly via a Mars van Krevelen mechanism<sup>32</sup>. Although that is the first time to our knowledge that such an hypothesis is proposed, the partial oxidation of organic products over CoO in reducing environment is not so wacky: on the one hand, cobalt oxides have indeed already been reported as efficient catalysts for partial oxidation of hydrocarbons<sup>33</sup>; on the other hand, selective oxidation of organic products in the absence of oxygen has also already been evidenced over other catalysts such as perovskite oxides<sup>34</sup>. Heavy unsaturated hydrocarbons with high boiling points and desorbing hardly from active sites are most likely good candidates for the sacrificial hydrogenation of CoO leading to even heavier and strongly

adsorbed oxygenates which could subsequently contribute to catalyst deactivation by blocking access to active sites.

Note that the hypothesis of a partial oxidation of hydrocarbons by CoO is proposed here as a specific explanation for the formation of strongly adsorbed oxygenate species. Gaseous oxygenate products, even if present in a minor extent in the present case (selectivity < 2%), can still be formed via more classical mechanisms involving CO insertion<sup>3-4</sup>.

Finally, if CoO is really responsible for most of oxygenate species formation, it would be therefore recommended to modify the activation step by reducing the catalyst at a higher temperature so that the catalyst contains no more CoO or at least as less as possible before Fischer-Tropsch synthesis. However, high reduction temperatures being known to favor sintering, it could be rather recommended to promote cobalt catalysts with a metal enhancing cobalt reducibility such as platinum<sup>35</sup>.

## Conclusions

The Fischer-Tropsch synthesis was investigated over a Co/Al<sub>2</sub>O<sub>3</sub> catalyst by the means of an innovative XRD-DRIFTS prototype which was optimally designed to carry out the reaction in representative conditions while monitoring simultaneously the structure and the surface of the catalyst. *Operando* XRD characterization clearly showed that the catalyst was further reduced during the first days of the reaction, the residual CoO being converted into face-centered cubic cobalt and crystallographic defects. At low CO conversion, thus low water partial pressure, CoO reduction was dominant over Co oxidation. Unfortunately, the better reduction degree did not generate a better activity. On the contrary, the conversion of CoO into Co was suspected to proceed via the reduction by hydrocarbons, generating their own partial oxidation. This hypothesis would explain the formation of strongly adsorbed oxygenate species at the surface of the catalyst, as observed on *operando* DRIFT spectra. Those species, as well as unsaturated species, could likely deposit on cobalt active sites and thus be responsible for most of the deactivation. From another side, DRIFT spectra also depicted the formation of carbonyls at the surface of the catalyst. Their decrease, associated with an increase in catalytic activity, was seen as an indirect evidence supporting the postulate that the Fischer-Tropsch main mechanism requires CO dissociation. These results also support the idea of a surface reconstruction, which was seen in this work as an activating phenomenon, with a beneficial effect on activity, rather than a deactivation origin as often focused on. This *avant-garde operando* XRD-DRIFTS study allowed obtaining a wealth of information stimulating discussion and leading to new insights in better understanding some of the interdependent complex phenomena occurring during Fischer-Tropsch synthesis.

## Acknowledgements

The INEL company is acknowledged for its implication in the development of the XRD-DRIFTS prototype. The French government and French citizens are thanked for their contribution in financing IFPEN.

## References

- 1 P. R. Ellis, D. James, P. T. Bishop, J. L. Casci, C. M. Lok, G. J. Kelly, in: B. H. Davis, M. L. Occelli (Eds.), *Advances in Fischer-Tropsch Synthesis, Catalysts, and Catalysis*, CRC Press, Boca Raton, 2010, p. 403.
- 2 A. R. De la Osa, A. De Lucas, J. Diaz-Maroto, A. Romero, J. L. Valverde, P. Sanchez, *Catal. Today* 187 (2012) 173.
- 3 A. De Klerk, *Fischer-Tropsch Refining*, John Wiley & Sons, 2011, p. 620.
- 4 R. A. Van Santen, I. M. Ciobica, E. Van Steen, M. M. Ghouri, in: B. C. Gates, H. Knözinger (Eds.), *Advances in Catalysis* 54, Academic Press, Burlington, 2011, p. 339.
- 5 A. M. Saib, D. J. Moodley, I. M. Ciobica, M. M. Hauman, B. H. Sigwebela, C. J. Weststrate, J. W. Niemantsverdriet, J. Van de Loosdrecht, *Catal. Today* 154 (2010) 271.
- 6 P.J. Van Berge, J. Van de Loosdrecht, S. Barradas, A. M. Van der Kraan, *Catal. Today* (2000), 321.
- 7 J. Van de Loosdrecht, B. Balzhinimayev, J. A. Dalmon, S. V. Niemantsverdriet, S. V. Tsybulya, A. M. Saib, P. J. Van Berge, J.L. Visagie, *Catal. Today* 123 (2007) 293.
- 8 G. L. Bezemer, T. J. Remans, A. P. Van Bavel, A. I. Dugulan, *J. Am. Soc.* 132 (2010) 8540.
- 9 J. Scalbert, C. Legens, I. Clémençon, A. L. Taleb, L. Sorbier, F. Diehl, *Chem. Comm.* 50 (2014) 7866.
- 10 H. Schulz, Z. Nie, F. Ousmanov, *Cat. Today* 71 (2002) 351.
- 11 F. C. Meunier, *Chem. Soc. Rev.* 39 (2010) 4602.
- 12 J. Scalbert, F. C. Meunier, C. Daniel, Y. Schuurman, *Phys. Chem. Chem. Phys.* 14 (2012) 2159.
- 13 L. Braconnier, E. Landrivoon, I. Clémençon, C. Legens, F. Diehl, Y. Schuurman, *Catal. Today* 215 (2013) 18.
- 14 J. P. Den Breejen, P. B. Radstake, G. L. Bezemer, J. H. Bitter, V. Froseth, A. Holmen, K. P. De Jong, *J. Am. Chem. Soc.* 131 (2009) 7197.
- 15 E. Iglesia, *Appl. Catal. A* 161 (1997) 59.
- 16 W. Zhou, J. G. Chen, K. G. Fang, Y. H. Sun, *Fuel Process. Technol.* 87 (2006) 609.
- 17 A. R. De la Osa, A. De Lucas, A. Romero, J.L. Valverde, P. Sanchez, *Catal. Today* 176 (2011) 298.
- 18 V. Sanchez-Escribano, M. A. Larrubia Vargas, E. Finocchio, G. Busca, *Appl. Catal. A* 316 (2007) 68.
- 19 J. Coates, in: R. A. Meyers (Ed.), *Encyclopedia of Analytical Chemistry*, John Wiley & Sons, Chichester, 2011, p. 16504.
- 20 D. Lin-Vien, N. B. Colthup, W. G. Fateley, J. G. Grasselli, *The Handbook of Infrared and Raman Characteristic Frequencies of Organic Molecules*, Academic Press, San Diego, London, 1991, p. 503.
- 21 J. Scalbert, I. Clémençon, C. Legens, F. Diehl, D. Decottignies, S. Maury, *Oil Gas Sci. Technol.*, DOI: 10.2516/ogst/2014031.
- 22 G. Prieto, A. Martínez, P. Concepcion, R. Moreno-Tost, *J. Catal.* 266 (2009) 129.
- 23 D. Pena, A. Griboval-Constant, F. Diehl, V. Lecocq, A. Y. Khodakov, *Chem. Cat. Chem.* 5 (2013) 728.
- 24 G. Kadinov, C. Bonev, S. Todorova, A. Palazov, *J. Chem. Soc., Faraday Trans.* 94 (1998) 3027.
- 25 K. Hoydalsvik, J. B. Floystad, A. Voronov, G. J. B. Voss, M. Esmaeili, J. Kehres, H. Granlund, U. Vainio, J. W. Andreasen, M. Ronning, D. W. Breiby, *J. Phys. Chem. C* 118 (2014) 2399.
- 26 X. Q. Wang, *Phys. Rev. Lett.* 67, 25 (1991) 3547.

- 27 R. Koch, M. Borbonus, O. Haase, K. H. Rieder, *Appl. Phys. A* 55 (1992) 417.
- 28 G. A. Somorjai, J. Y. Park, *Chem. Soc. Rev.* 37 (2008) 2155.
- 29 A. Tuxen, S. Carenco, M. Chintapalli, C. H. Chuang, C. Escudero, E. Pach, P. Jiang, F. Brondics, B. Beberwyck, A. P. Alivisatos, G. Thornton, W. F. Pong, J. Guo, R. Perez, F. Besenbacher, M. Salmeron, *J. Am. Chem. Soc.* 135 (2013) 2273.
- 30 G. L. Bezemer, J. H. Bitter, H. P. C. E. Kuipers, H. Oosterbeek, J. E. Holewijn, X. Xu, F. Kapteijn, A. J. van Dillen, K. P. de Jong, *J. Am. Chem. Soc.* 128, 12 (2006) 3956.
- 31 N. Navidi, J.W. Thybaut, G.B. Marin, *Appl. Catal. A* 469 (2014) 357.
- 32 P. Mars, D. W. van Krevelen, *Spec. Suppl. To Chem. Eng. Sci.* 3 (1954) 41.
- 33 L. Li, H. Li, C. Jin, X. Wang, W. Ji, Y. Pan, T. Van der Knaap, R. Van der Stoel, C. T. Au, *Catal. Lett.* 136 (2010) 20.
- 34 R. Sumathi, K. Johnson, B. Viswanathan, T. K. Varadarajan, *Appl. Catal. A* 172 (1998) 15.
- 35 F. Diehl, A. Y. Khodakov, *Oil Gas Sci. Technol.* 64 (2009) 11.